

Formation of Oxide Phases in the System Pr-Fe-O

Ristić, Mira; Popović, Stanko; Musić, Svetozar

Source / Izvornik: **Croatica Chemica Acta, 2013, 86, 281 - 285**

Journal article, Published version

Rad u časopisu, Objavljena verzija rada (izdavačev PDF)

<https://doi.org/10.5562/cca2247>

Permanent link / Trajna poveznica: <https://um.nsk.hr/um:nbn:hr:217:789321>

Rights / Prava: [Attribution 4.0 International](#)/[Imenovanje 4.0 međunarodna](#)

Download date / Datum preuzimanja: **2024-08-08**



Repository / Repozitorij:

[Repository of the Faculty of Science - University of Zagreb](#)



Formation of Oxide Phases in the System Pr-Fe-O

Mira Ristić,^{a,*} Stanko Popović,^b and Svetozar Musić^a

^a*Ruđer Bošković Institute, Bijenička cesta 54, P. O. Box 180, Zagreb, HR-10002, Croatia*

^b*Department of Physics, Faculty of Science, University of Zagreb, Zagreb, HR-10000, Croatia*

RECEIVED MARCH 8, 2013; REVISED JULY 22, 2013; ACCEPTED SEPTEMBER 2, 2013

Abstract. The formation of oxide phases at 900 °C in the system Fe₂O₃-“Pr₂O₃” was investigated. With a decrease in the molar fraction of Fe₂O₃ a corresponding increase in PrFeO₃ was observed. For equal molar fractions of Fe₂O₃ and “Pr₂O₃” the formation of PrFeO₃ and very small fractions of α-Fe₂O₃ plus an additional oxide phase, which could not be identified with certainty, were observed. With further increase in “Pr₂O₃” fraction the praseodymium oxides Pr₆O₁₁ and PrO₂ started to become dominant in the phase composition. The small fraction (< 0.02) of the same unidentified oxide phase was also obtained when Pr(OH)₃ was calcined in air at 900 °C; this was probably a mixture of other praseodymium oxides with different average oxidation numbers of Pr. The results of XRD, ⁵⁷Fe Mössbauer and FT-IR spectroscopies are discussed. (doi: [10.5562/cca2247](https://doi.org/10.5562/cca2247))

Keywords: α-Fe₂O₃, PrFeO₃, praseodymium oxides

INTRODUCTION

RE-orthoferrites (RE = rare earth) and their substituted compounds are in the focus of many studies due to their specific magnetic, electrical and chemical properties. These materials have potential applications in solid-state fuel cells, catalysis or as various types of sensors. The microstructural properties of RE-orthoferrites can be changed by the synthesis route or substitution of Fe with selected metal cations.

Rajendran *et al.*¹ prepared thin films of selected RE-orthoferrites on fused silica using sol-gel processing combined with calcination at 650 °C. Sivakumar *et al.*² prepared nanocrystalline orthoferrites GdFeO₃, ErFeO₃, TbFeO₃ and EuFeO₃ starting from Fe(CO)₅ and corresponding RE-carbonate with the aid of sonochemistry. The orthoferrite precursors were then calcined between 800 and 910 °C for 24 h in air atmosphere. Rajendran and Bhattacharya³ reported the formation of nanocrystalline orthoferrite powders of selected RE cations combining the coprecipitation and calcination of the gel precursor at 650 to 700 °C in air. The coprecipitation method was also used⁴ to prepare DyFeO₃. To a solution of DyCl₃ and FeCl₂ salts NaOH solution was added, the coprecipitate was washed and dried, then heated in air at 700 to 1000 °C. In this temperature range XRD showed

the formation of a DyFeO₃ phase. RE-orthoferrites of La, Pr and Nd were synthesized at 400 °C using a molten NaOH flux.⁵ Li *et al.*⁶ prepared RE orthoferrites (RE = La, Pr-Tb) in the form of hollow spheres or solid spheres (RE = Dy-Yb, Y) using the calcination of the RE-Fe citrate complex at ~ 800 °C. All these RE-orthoferrites were successfully used for catalytical reduction of NO pollutant by CO at 200 to 500 °C and their efficiency could be compared with noble metal catalysts. The effect of Ca²⁺ substitution on the structural and magnetic properties of RE-orthoferrite was investigated.⁷ Also, (RE)_{0.7}Ca_{0.3}FeO₃, RE = La, Dy, Y, Er or Gd were investigated for possible applications as pressure or γ-ray sensor.⁸ The structural, morphological and transport properties influenced by doping Ni for Fe in PrFeO₃ ceramic thin films were investigated as well.⁹ Saraswat *et al.*¹⁰ prepared the hydroxide coprecipitate Fe(OH)₃/Pr(OH)₃ containing Fe(III) (*w* = 5 %). The coprecipitate was heated up to 1100 °C. In the present work we extended the investigation of the system Fe₂O₃-“Pr₂O₃” by varying the molar fractions of Fe₂O₃ and “Pr₂O₃” with the aim to identify the actual crystal phases formed in this mixed oxides system. Praseodymium has a much more complex oxide chemistry than the other rare earths and this is probably one of the reasons why the formation of PrFeO₃ has been less investigated.

* Author to whom correspondence should be addressed. (E-mail: ristic@irb.hr)

Table 1. XRD analysis of the samples prepared in the system Fe₂O₃-“Pr₂O₃” where “Pr₂O₃” is virtual composition and X is unknown phase

| Sample | Initial (molar) ratio Fe ₂ O ₃ -“Pr ₂ O ₃ ” | Phase composition as found by XRD (approx. molar fraction in brackets) |
|--------|--|---|
| S1 | 99 : 1 | α -Fe ₂ O ₃ + PrFeO ₃ (0.02) |
| S2 | 97 : 3 | α -Fe ₂ O ₃ + PrFeO ₃ (0.06) |
| S3 | 95 : 5 | α -Fe ₂ O ₃ + PrFeO ₃ (0.1) |
| S4 | 90 : 10 | α -Fe ₂ O ₃ + PrFeO ₃ (0.2) |
| S5 | 85 : 15 | α -Fe ₂ O ₃ + PrFeO ₃ (0.3) |
| S6 | 80 : 20 | α -Fe ₂ O ₃ + PrFeO ₃ (0.4) |
| S7 | 70 : 30 | PrFeO ₃ + α -Fe ₂ O ₃ (0.4) |
| S8 | 50 : 50 | PrFeO ₃ + α -Fe ₂ O ₃ (~0.01) + X (< 0.02) |
| S9 | 30 : 70 | Pr ₆ O ₁₁ (\leq 1/2) + PrFeO ₃ (\leq 1/2) + PrO ₂ (0.05) + X (< 0.02) |
| S10 | 10 : 90 | Pr ₆ O ₁₁ + PrO ₂ (0.20) + PrFeO ₃ (0.10) + X (< 0.02) |
| S11 | “Pr ₂ O ₃ ” | Pr ₆ O ₁₁ ^(a) + PrO ₂ ^(b) + X (< 0.02) |

^(a) Identified according JCPDS PDF card No. 6-329^(b) Identified according JCPDS PDF card No. 24-1006

EXPERIMENTAL

Analytical grade chemicals, Fe(NO₃)₃ · 9 H₂O, Pr(NO₃)₃ · 6 H₂O and 25 % NH₃(aq), were used. Twice-distilled water was prepared in own laboratory. Mixed hydroxides Fe(OH)₃/Pr(OH)₃ were quantitatively coprecipitated by adding NH₄OH solution to an aqueous solution of Fe(NO₃)₃ + Pr(NO₃)₃ salts. The hydroxide coprecipitates were washed by centrifugation without permitting the peptization of the mixed hydroxide coprecipitate. After drying the coprecipitates were heated in air at 200 °C for 1 h, 400 °C for 1 h, 500 °C for 1 h, 600 °C for 1 h and 900 °C for 4 h. When the heating time was over, the crucibles were removed from the oven and cooled in air to room temperature (RT).

XRD patterns were recorded at RT using the Philips MPD 1880 diffractometer (Cu-K α radiation, graphite monochromator and proportional counter). ⁵⁷Fe Mössbauer spectra were recorded at 20 °C in the transmission mode using the spectrometer setup with WissEl (Starnberg, Germany) products. ⁵⁷Co in Rh matrix was used as Mössbauer source. The velocity scale and Mössbauer parameters refer to the metallic α -Fe absorber at 20 °C. The raw spectra were fitted using the MossWin program.

FT-IR spectra were recorded at RT with Perkin-Elmer spectrometer (model 2000). Powders were mixed with spectroscopically pure KBr and pressed into tablets using a Carver press. The particles were inspected with a JEOL thermal field emission scanning electron microscope (model JSM-7000F). The inspected particles were not coated with an electrically conductive layer.

RESULTS AND DISCUSSION

The results of XRD phase analysis of samples S1 to S11 with different initial molar ratios in the system Fe₂O₃-“Pr₂O₃” are given in Table 1. The oxides of α -Fe₂O₃ and PrFeO₃ phases were found in the samples prepared in the initial molar ratio α -Fe₂O₃:“Pr₂O₃” = 70:30 (samples S1 to S7). The phase analysis of sample S8 prepared from equal initial molar ratios of Fe₂O₃ and “Pr₂O₃” showed the formation of PrFeO₃ and a very small fraction of α -Fe₂O₃ (~0.01) plus an undetermined phase X (< 0.02). With an increase in the heating temperature up to 1100 °C the orthoferrite PrFeO₃, as a single phase, is formed. With further increase in the starting “Pr₂O₃” fraction there is a corresponding decrease in the PrFeO₃ fraction accompanied by the appearance of praseodymium oxide phases, Pr₆O₁₁ and PrO₂. The Pr₆O₁₁, PrO₂ and X (< 0.02) phases were obtained when only the Pr(OH)₃ precursor was used (sample S11). The fraction X (< 0.02) was not identified with certainty due to very small intensities of diffraction lines and possible overlapping of several other praseodymium oxides. Apart from Pr₂O₃ with oxidation number Pr³⁺ and PrO₂ with oxidation number Pr⁴⁺ there were several other praseodymium oxides with varying average oxidation numbers such as Pr₇O₁₂, Pr₉O₁₆, Pr₅O₉, Pr₁₁O₂₀ and Pr₆O₁₁.¹¹ The formation of these oxide phases depends on the maximum heating temperature, annealing and the cooling atmosphere. In this respect the oxide chemistry of praseodymium is specific among other rare earth elements. More about the stoichiometry of praseodymium oxides is reported in selected references.¹²⁻¹⁵

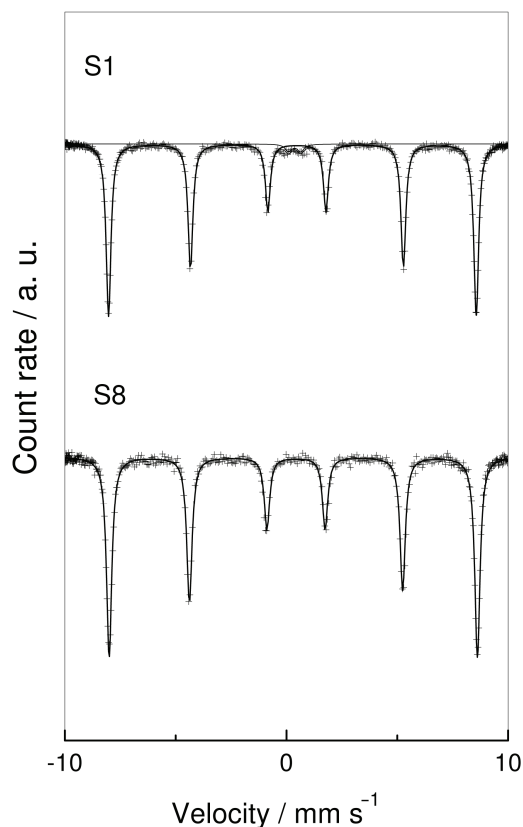


Figure 1. ^{57}Fe Mössbauer spectra of samples S1 and S8, recorded at 20 °C.

Figure 1. shows the Mössbauer spectra of the selected samples (S1 and S8), whereas the calculated Mössbauer parameters for all Fe-containing samples are given in Table 2. RT Mössbauer spectra of $\alpha\text{-Fe}_2\text{O}_3$ and PrFeO_3 showed magnetic hyperfine structure (MHS) with similar Mössbauer parameters. For that reason these two hyperfine magnetically splitted subspectra were fitted as one sextet. The presence of the PrFeO_3 phase in dependence on a decrease in the $\alpha\text{-Fe}_2\text{O}_3$ fraction can be monitored only on the basis of changes in quadrupole splitting, as clearly discernible in Table 2.

The Mössbauer spectrum of sample S1 showed the superposition of one sextet (M) and one central quadrupole doublet (Q) of small relative intensity. The parameters of sextet M corresponds to $\alpha\text{-Fe}_2\text{O}_3$ phase.¹⁶ Taking into account the results of XRD measurement the central quadrupole doublet Q can be assigned to very fine PrFeO_3 crystallites. The dissolution of Pr^{3+} cation into $\alpha\text{-Fe}_2\text{O}_3$ crystal structure is not likely, due to a great difference in the ionic radii of Fe^{3+} and Pr^{3+} cations. Samples S2 to S8 show only one sextet which is actually a superposition of two sextets with similar parameters. Eibschütz *et al.*¹⁷ measured the Mössbauer spectra of different RE-orthoferrites including PrFeO_3 . At 296 K, the following parameters for PrFeO_3 were measured: HMF = 51.0 T and Eq = 0.012

Table 2. Calculated Mössbauer parameters at 20 °C, where δ is isomer shift; Δ or Eq is quadrupole splitting; HMF is hyperfine magnetic field. Isomer shift, δ , is given relative to $\alpha\text{-Fe}$ at 20 °C.

| Sample | Line | $\delta^{(a)}$ / mm s^{-1} | Δ or Eq ^(b) / mm s^{-1} | HMF ^(c) / T | Γ / mm s^{-1} | Area/ % |
|--------|------|--|---|---------------------------|----------------------------------|------------|
| S1 | M | 0.37 | -0.20 | 51.5 | 0.26 | 97.4 |
| | Q | 0.37 | 0.55 | – | 0.35 | 2.6 |
| S2 | M | 0.37 | -0.20 | 51.5 | 0.27 | 100 |
| S3 | M | 0.37 | -0.19 | 51.5 | 0.27 | 100 |
| S4 | M | 0.37 | -0.19 | 51.5 | 0.27 | 100 |
| S5 | M | 0.37 | -0.17 | 51.5 | 0.28 | 100 |
| S6 | M | 0.37 | -0.17 | 51.5 | 0.28 | 100 |
| S7 | M | 0.37 | -0.14 | 51.4 | 0.27 | 100 |
| S8 | M | 0.37 | -0.12 | 51.4 | 0.27 | 100 |
| S9 | M | 0.37 | -0.04 | 51.2 | 0.27 | 100 |
| S10 | M | 0.37 | -0.02 | 51.2 | 0.27 | 100 |

^(a) Error $\delta = \pm 0.01 \text{ mm s}^{-1}$

^(b) Error Δ or Eq = $\pm 0.01 \text{ mm s}^{-1}$

^(c) Error HMF = $\pm 0.2 \text{ T}$

mm s^{-1} . Saraswat *et al.*¹⁰ measured RT Mössbauer parameters for PrFeO_3 : HMF = 50.6 T and Eq = 0.06 mm s^{-1} . A difference in Mössbauer parameters for PrFeO_3 can be assigned to different ways of the formation of this orthoferrite. Pasternak *et al.*¹⁸ investigated the high-pressure (HP) structural, magnetic and electronic properties of RE-orthoferrites with the large (La^{3+} , Pr^{3+}), the intermediate (Eu^{3+} , Y^{3+}) or the smallest Lu^{3+} cations. PrFeO_3 subjected to high pressure shows two equally abundant magnetic sublattices due to high-spin and low-spin Fe^{3+} sites. Starting with 40 GPa the RT Mössbauer spectra show a superposition of two central quadrupole doublets. The quadrupole doublet with smaller Δ and δ corresponds to the HS sublattice. By cooling PrFeO_3 to 5 K both high-spin (HS) and low-spin (LS) subspectra become magnetically ordered.¹⁸

FT-IR spectra of samples S1 to S10 also show gradual changes in dependence on the initial molar ratio Fe_2O_3 : “ Pr_2O_3 ”. The spectrum of sample S1, shown in Figure 2., can be assigned to the hematite phase. Hematite (D_{3d}^6 symmetry) is characterized by six IR active vibrations, two A_{2u} ($E||C$) and four E_u ($E\perp C$).^{19,20} In the present case, for sample S1 these vibrations were recorded at 630 cm^{-1} (A_{2u}), 550 cm^{-1} (E_u), 475 cm^{-1} (E_u), 390 cm^{-1} (A_{2u}) and 344 cm^{-1} (E_u). Different factors, such as crystallinity, size and morphology of hematite particles determine the positions of the corresponding IR bands. With an increase in “ Pr_2O_3 ” molar fraction the IR band at 630 cm^{-1} , as well as IR band at 390 cm^{-1} are diminishing. The FT-IR spectrum of sample S8 with PrFeO_3 molar fraction larger than 0.97, as found with XRD, shows

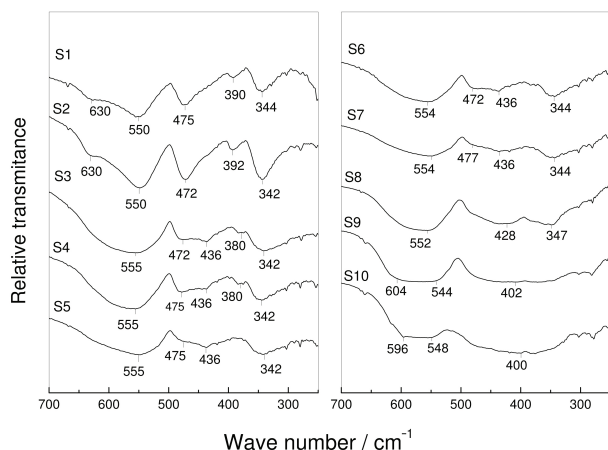


Figure 2. FT-IR spectra of samples S1 to S10, recorded at RT.

three IR bands positioned at 552, 428 and 347 cm^{-1} . Two strong IR bands at $\sim 560 \text{ cm}^{-1}$ and $\sim 440 \text{ cm}^{-1}$ were recorded for EuFeO_3 , GdFeO_3 , TbFeO_3 and ErFeO_3 .² The IR band at $\sim 560 \text{ cm}^{-1}$ was assigned to the Fe–O stretching vibration, whereas the $\sim 440 \text{ cm}^{-1}$ band was interpreted as O–Fe–O deformation vibration. Sivakumara⁵ recorded the IR bands at 562, 421 and 381 cm^{-1} for PrFeO_3 , similar to the case of LaFeO_3 .²¹ The appearance of two IR bands at 421 and 381 cm^{-1} , corresponding to the O–Fe–O deformation vibration, was explained as a deviation from the ideal RE-orthoferrite crystal structure. FT-IR spectrum of sample S10 showed two very broad IR bands positioned at 596–548 and 400 cm^{-1} . In line with XRD analysis it can be concluded that the Pr–O and O–Pr–O vibrations of Pr_6O_{11} and PrO_2 predominantly contribute to this FT-IR spectrum.

Figure 3. shows FE-SEM images of selected samples S1 and S8. The image of sample S1 shows micron and submicron hematite particles (Figure 3a.). The image of sample S8 also shows similar PrFeO_3 particles (Figure 3b.). EDS analysis (Figure 4.) of selected area of sample S8 shows the atomic ratio Pr:Fe close to the ratio in PrFeO_3 in line with the nominal chemical composition shown in Table 1.

CONCLUSION

Formation of oxide phases in the system Pr–Fe–O at 900 °C was monitored. The molar fraction of PrFeO_3 increased with increase of the starting molar fraction “ Pr_2O_3 ”. PrFeO_3 and small amounts of $\alpha\text{-Fe}_2\text{O}_3$ and unidentified oxide phase(s) were formed when equal molar fractions of Fe_2O_3 and “ Pr_2O_3 ” were used. With further increase in the molar fraction of “ Pr_2O_3 ”, Pr_6O_{11} and PrO_2 started to become dominant in the phase composition. The small fraction (< 0.02) of the same unidentified phase was also obtained upon the calcination of pure $\text{Pr}(\text{OH})_3$ precipitate up to 900 °C. It was suggested that this unidentified oxide phase is very proba-

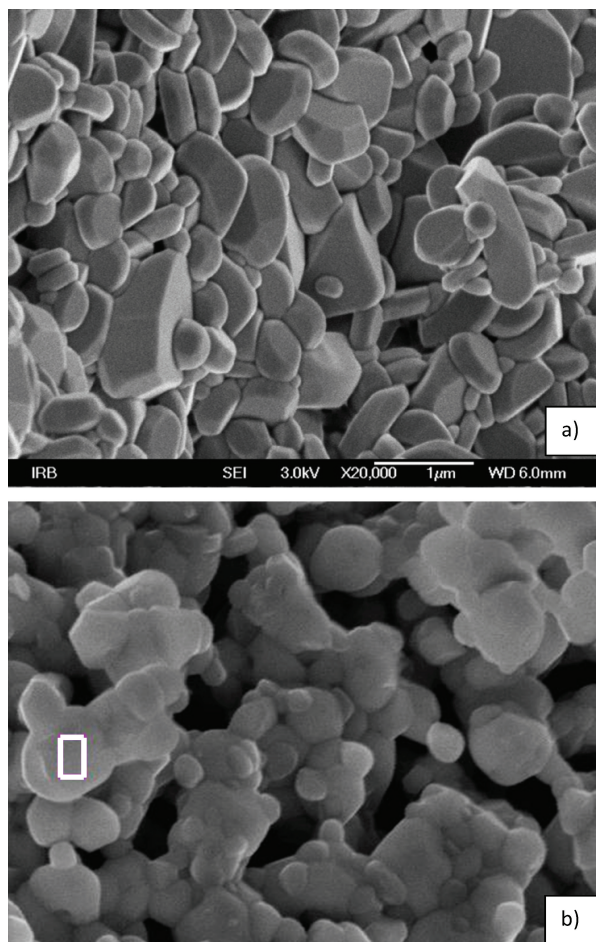


Figure 3. FE-SEM images of samples S1 (a) and S8 (b).

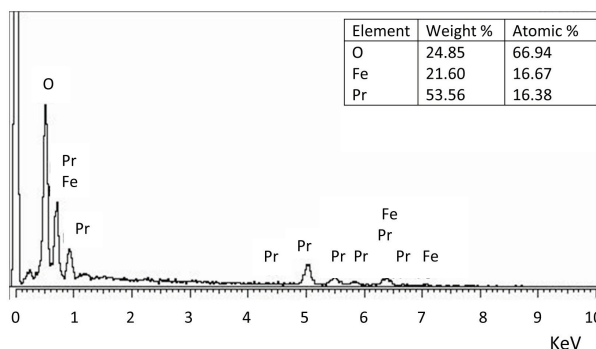


Figure 4. EDS spectrum of the particle in sample S8 (selected area in Figure 3b.).

bly a mixture of other praseodymium oxides with different average oxidation numbers of Pr.

REFERENCES

1. M. Rajendran, M. Ghanashyam Krishna, and A. K. Bhattacharya, *Thin Solids Films* **385** (2001) 230–233.
2. M. Sivakumar, A. Gedanken, D. Bhattacharaya, I. Brukental, Y. Yeshurun, W. Zhong, Y. W. Du, I. Felner, and I. Nowik, *Chem. Mater.* **16** (2004) 3623–3632.

3. M. Rajendran and A. K. Bhattacharya, *J. Eur. Ceram. Soc.* **26** (2006) 3675–3679.
4. L. Zhu, N. Sakai, T. Yanoh, S. Yano, N. Wada, H. Takeuchi, A. Kurokawa, and Y. Ichianagi, Proceedings of Asia Pacific Interdisciplinary Research Conference 2011. *J. Physics: Conference Series* **352** (2012) 012021.
5. C. Shivakumara, *Solid State Commun.* **139** (2006) 165–169.
6. X. Li, C. Tang, M. Ai, L. Dong, and Z. Xu, *Chem. Mater.* **22** (2010) 4879–4889.
7. M. A. Ahmed, S. I. El-Dek, *Mater. Sci. Eng. B* **128** (2006) 30–33.
8. M. A. Ahmed, S. I. El-Dek, *Mater. Lett.* **60** (2006) 1437–1446.
9. F. A. Mir, M. Ikram, and R. Kumar, *Philosoph. Magazine* **92** (2012) 1058–1070.
10. I. P. Saraswat, A. C. Vajepi, V. K. Garg, and Nam Prakash, *J. Mater. Sci.* **16** (1981) 433–438.
11. S. Ferro, *Int. J. Electrochem.* **2011** (2011) Article ID 561204.
12. F. J. Lincoln, J. R. Sellar, and B. G. Hyde, *J. Solid State Chem.* **74** (1988) 268–276.
13. Z. C. Kang, L. Eyring, *J. Solid State Chem.* **75** (1988) 52–59.
14. R. Sharma, H. Hinode, and L. Eyring, *J. Solid. State Chem.* **92** (1991) 401–419.
15. L. Eyring, *J. Alloys Comp.* **207/208** (1994) 1–19.
16. E. Murad, J. H. Johnston, *Iron Oxides and Oxyhydroxides*, in G. J. Long (Ed.) *Mössbauer Spectroscopy Applied to Inorganic Chemistry*, Vol. 2, Plenum Publ. Corp., NY, 1987, pp. 507–582.
17. M. Eibschütz, S. Shtrikman, and D. Treves, *Phys. Rev.* **156** (1967) 562–577.
18. M. P. Pasternak, W. M. Xu, G. Kh. Rozenberg, and R. D. Taylor, *Electronic, Magnetic and Structural Properties of the RFeO₃ Antiferromagnetic-Pervoskites at Very High Pressures*, Report LA-UR-02-2720, Edited by Los Alamos National Laboratory, University of California, USA
19. O. Onari, T. Arai, and K. Kudo, *Phys. Rev. B* **16** (1977) 1717–1721.
20. J. L. Rendon, J. Cornejo, P. De Arambarri, and C. J. Serna, *J. Coll. Interface Sci.* **92** (1983) 508–516.
21. W. Zheng, R. Liu, D. Peng, and G. Meng, *Mater. Lett.* **43** (2000) 19–22.